Project Number: PH GSI-0807

EXPERIMENTS WITH A THERMOACOUSTIC REFRIGERATOR

A Major Qualifying Project Report:
Submitted to the Faculty
of the
WORCESTER POLYTECHNIC INSTITUTE
in partial fulfillment of the requirements for the
Degree of Bachelor of Science
by

_____

Vineet Barot

_____

David Coit

Date: April 30, 2009

Approved:

_____

Professor Germano S. Iannacchione, Advisor

Abstract

Experiments were conducted on a reconstructed thermoacoustic refrigerator. The construction utilized the design and various reusable components from a previous major qualifying project. In addition, different materials were used as well as different methods with which to test the thermoacoustic effect. The effect was not observed due to failures in construction; and, the analysis of findings also put the previous project's conclusion of observing a thermoacoustic effect as well as the overall design into question.

Acknowledgments

Our deep gratitude goes to Professor Iannacchione for his advisory and wisdom during the many tolling hours put into this project. Also, we express a very special thanks to Roger Steele for his aide in the arduous setup of this experiment. We would also like to thank Nihar Pradhan and other graduate students of Olin Hall 004 for their general assistance with laboratory equipment.

Contents

List of Table and Figures

Introduction

Background

Refrigeration in thermodynamics refers to a cycle in which heat is pumped out of a system by doing work on it. Conventional refrigerators use a working fluid that absorbs the heat out of a chamber by using phase transitions. Thermoacoustic refrigeration uses sound waves to transfer heat from one area to another; thereby carrying heat away from a system to an exhaust. After a brief history of the field, the thermoacoustic effect is explained in more detail. The Introduction section ends with an explanation of the project and personal goals.

A Brief History

The effects of thermoacoustics have been observed for centuries. Specifically, glassblowers could hear the sounds created by thermal energy converting to acoustic energy when plying a temperature change to hot glass bulbs. Nikolaus Rott and other scientists such as Lord Rayleigh, coined “thermoacoustics” as it became understood that thermal and acoustical energies could transition between each other. However, it wasn’t until recently that this property has been explored for possible engineering applications which use its principles.

Heat can be produced from sound waves. The concept of “thermoacoustic” forms naturally when thinking about sound and temperature. Both phenomena involve the oscillation of particles. Sound is a pressure wave that transfers kinetic energy from one air molecule to the next using compression and expansion of the medium; and, temperature measures average kinetic energy of particles in a volume. By manipulating sound waves, it is fairly simple, at least in principle, to produce heat.

Since the early 1980’s, places like Los Alamos National Laboratory have been conducting experiments in the hopes of creating a device that has passive acoustical-phasing mechanisms.

The research continued through the works of Greg Swift and others whose work was later used by M. Tijani and others to develop a practical refrigerator. In 2004, Pennsylvania State University scientists Robert Smith, Steven Garret and Matt Poese developed a working refrigerator for Ben and Jerry's Ice Cream

(http://www.acs.psu.edu/thermoacoustics/refrigeration/benandjerrys.htm).

Today, thermoacoustic refrigerators are being researched for their practicality and because they're environmentally friendlier than conventional refrigerators because of their chemical independence.

Thermoacoustic Refrigeration Summarized

A conventional refrigerator has the working fluid in a circuit. At one part of the circuit is a motorized compressor which does work on the gas, compressing it and increasing the temperature to higher than that of its surroundings, such that it gives off heat. This high pressure fluid is transported along the outside of the controlled system (the refrigerated box) and to an expansion valve which adiabatically expands the fluid until it is colder than the box, such that it absorbs heat. The cooled fluid returns to the compressor where the process then begins again.

A thermoacoustic device uses a fluid medium (in our case Helium gas) to do work within the stack. The stack is a chamber with numerous linear sub-chambers connected to both ends where there are heat exchangers, one for hot and one for cold thermal energy. The sub-chambers are divided by plates whose spatial distances determine the area of heat flux caused by the working fluid. The fluid itself undergoes compression and expansion as it moves about these tunnels as a result of the sound waves passing. Given the correct frequency and

wavelength of sound waves, the hot heat energy will be transported to one side of the stack and the cold heat to another, which allows for a refrigeration process.

The basic components of the thermoacoustic refrigerator are the resonator, the stack, and the acoustic driver. Each component will be discussed in further detail in the design and materials sections.

Preceding Projects

There were two previous projects by WPI students. The first project was submitted in 2002 and the second by Andrew Lingenfelter and Megan LaBounty in 2008. Based on the design ideas of Tijani, Labounty and Lingenfelter built a working apparatus that had a maximum of 7K temperature difference across the stack; demonstrating thermoacoustic refrigeration. Due to specific project goals and time constraints, they were not able to develop the project further. Our project is a continuation of their experiments.

Our Goals and Intentions

The previous project concluded that the temperature difference they achieved, 7 Kelvin, was due to a thermoacoustic effect. By adjusting several key parameters, the current apparatus can be driven to pump more heat from the cold heat exchanger.

The first adjustable parameter is pressure. It has been proven that the temperature difference across stacks can be increased (to a certain extent) by increasing the internal average pressure (Tijani, 51). For Helium, Tijani et. al. recommend a maximum pressure of 12 atms (Tijani, 51). Previously, the refrigerator could sustain about 1.5 atms. In order to maintain higher pressure, many aspects of the experiment would have to be altered, namely the construction materials used.

Another upgradeable parameter is acoustic power. This is especially true if the refrigerator sustains greater pressures but, a more powerful speaker would be an advantage in itself. We acquired a microphone more suitable for this kind of setup for resonance testing and thermocouples that could be attached permanently for continuous temperature measurement. Measuring resonance of the system gave us the operating frequency with which to run the device.

By changing these parameters, the refrigerator will likely become more powerful (achieve a higher delta T) and perhaps more efficient.

Physical Principles

The thermoacoustic effect acts like a conveyor belt for thermal energy. For this to occur, one must exploit two physical principles concerning thermodynamics and acoustics inside the stack. First, through the relation of pressure to temperature by the ideal gas law PV=nRT, the small changes in pressure caused by sound also cause small changes in temperature. Secondly, if the gas through which the sound travels is near a solid surface, the gas may interact by transferring heat to and from it. Combining these two factors, we can create a four-step process similar to a Carnot cycle.

Thermoacoustic cycle consists of four steps. Figures 1-4 below show the steps with a piston as the acoustical driver (Tijani, p.6). Suppose there is gas trapped in a parallel stack of solid plates and there is an acoustic driver that sends a standing wave through the fluid with a pressure node and anti-node at either end of the stack. The first step in the thermoacoustic process is the translational movement and compression of a packet of gas, adiabatically, in one direction away from the pressure anti-node.

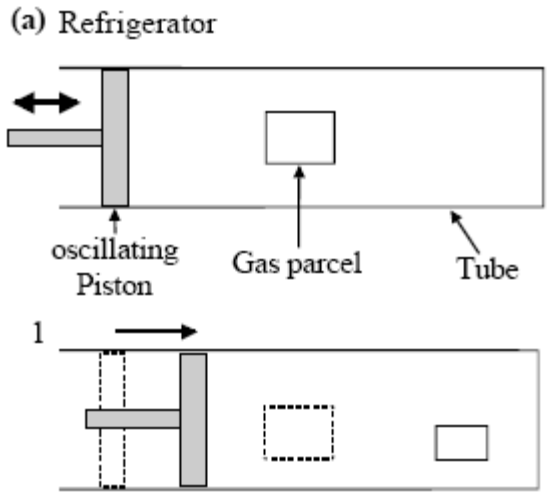

Figure 1 The first step of a thermoacoustic cycle.

This compression of the gas heats it up, so that the local surface will isobarically absorb some of the thermal energy.

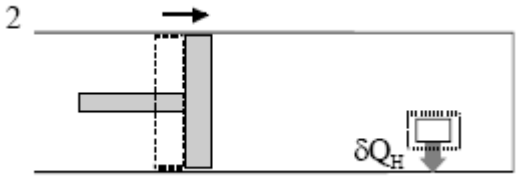

Figure 2 The second step of the thermoacoustic refrigeration.

The gas then adiabatically moves back and expands towards the pressure anti-node in the third step where then it isobarically absorbs heat from another surface area in the last step.

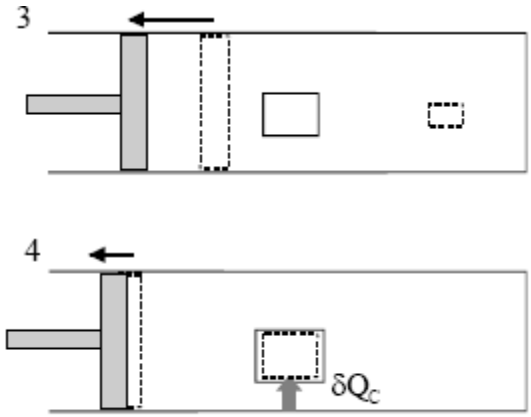

Figure 3 Steps 3 and 4 in the thermoacoustic cycle.

The oscillatory pattern repeats and heat is thus transferred, like a conveyor belt, from one side of the stack to the other. Over a long period time, the small amounts of heat displaced from one end to the other add together and cause a larger temperature difference.

Any geometric stack has a thermal penetration depth given by equation 1.

$$\delta_k = \sqrt{2f/\rho C w} \quad (1)$$

which denotes how quickly the fluid volume loses heat energy along the stack's longitudinal axis. Similarly, the viscous penetration depth

$$\delta_v = \sqrt{2v/w} \quad (2)$$

where v = μ/ρ (kinematic viscosity equals the dynamic viscosity over the fluid density) determines the effect of the fluid viscosity along the melinex wrap. Solving for these two depths will yield the Prandtl number $\sigma = (\delta_v/\delta_k)^2$ of the geometric stack and will determine how much energy the oscillating particles will deposit each cycle.

The acoustic power of the device,

$$W_A = p_m a A \quad (3)$$

of mean pressure p_m, speed of sound a, cross-sectional area A, has a power density dependent on the resonance produced by the small tube resonator. To achieve the appropriate resonance, the wavenumber k must be selected from the optimization of the resonance condition

$$\cot(kl) = (D_1/D_2)^2 \tan(k(L_t - l)) \quad (4)$$

where l is the length of the large diameter tube, L_t is the length of the total resonator including the stack and large diameter tube, and $D_{1,2}$ is the diameter of the small and large diameter tubes, respectively. For convenience, we did not calculate the wavenumber mathematically and instead used a microphone to test for resonance peaks, as will be shown later. Equations 1 through 4 are taken from Tijani et. Al. (Tijani, pg.50, 55).

The sound waves generated by the driver all follow the wave equation:

$$\lambda/T = v(p) \quad (5)$$

this is the phase velocity of the standing wave equal to the wavelength over the period. Phase velocity v(p) also equals w/k, where angular frequency $w=2\pi f$, period $T=2\pi/w$, and k is the wavenumber. Using this, we can calculate where pressure nodes and anti-nodes will be for the placement of the stack.

For this construction L_t was 63 +/- 2 cm, the stack itself was 8.33 +/- .03 cm, and the length of the large diameter tube, l, was 15 +/- 1 cm.

The design of the refrigerator was based around Tijani's design which was based on a frequency of around 400 Hz in Helium. The following calculations show how the resonator length was determined using this frequency. The speed of sound in helium from the equation,

$$v_s = \sqrt{\gamma RT/M} \quad (6)$$

where M is the molecular mass of helium at .004 kg/mol, which turns out to be 1020 +/- 80 m/s at a temperature of about 23 +/- 2 ^{0}C (300K). Using this as our phase velocity and dividing by Tijani's frequency, 400 1/s, achieved during resonance testing, the wavelength turns out to be 2.6 +/- 0.2 m. The length of the resonator should be either $\lambda/2$ for a closed end tube or $\lambda/4$ for a tube with an open end. The latter being preferable because it reduces power loss from extra surface area, so that there can be a standing wave "bounced" off the open buffer volume, which acts as a pressure node (Tijani, p.55). Using the above value for wavelength, the length of the entire resonator L_t should thus be 63 cm which matches the measured value.

Combining acoustic principals and heat transfer, the general equation for relating the temperature difference of pressure waves is,

$$T_1/T_m = (\gamma\text{-}1/\gamma)\ (p_1/p_m)\ (7)$$

where T_m and p_m are the mean temperature and pressure within the stack and T_1, p_1 are the temperature and pressure differences between one edge of the stack and the mean (i.e. $2T_1$ is the total temperature difference and $2p_1$ is total pressure difference between the two sides). After receiving temperature data and knowing the pressure input of helium into the system, the pressure wave p_1 can be calculated.

One more set of equations worth mentioning, yet is not used, is the Rott wave equation of thermoacoustics modified by G.W. Swift. Thermoacoustics is generally a very complicated phenomenon and, to date, there is limited mathematical modeling. Figure 4 show the stack equations for the wave function and temperature gradient created in the parallel plates.

$$\left(1+\frac{(\gamma-1)f_\kappa}{1+\varepsilon_s}\right)p_1+\frac{\rho_m a^2}{\omega^2}\frac{d}{dx}\left(\frac{1-f_v}{\rho_m}\frac{dp_1}{dx}\right)-\beta\frac{a^2}{\omega^2}\frac{f_\kappa-f_v}{(1-\sigma)(1+\varepsilon_s)}\frac{dT_m}{dx}\frac{dp_1}{dx}=0$$

$$f_v=\frac{\tanh[(1+i)y_0/\delta_v]}{(1+i)y_0/\delta_v}$$

$$f_\kappa=\frac{\tanh[(1+i)y_0/\delta_\kappa]}{(1+i)y_0/\delta_\kappa}$$

$$\varepsilon_s=\frac{\sqrt{K\rho_m c_p}\tanh[(1+i)y_o/\delta_\kappa]}{\sqrt{K_s\rho_s c_s}\tanh[(1+i)y_o/\delta_s]}$$

$$\sigma=c_p\mu/K=\nu/\kappa$$

Figure 4. Thermoacoustic equations. http://mshades.free.fr/

Primary and Alternate Design

The previous group constructed their refrigerator using the design of M.E.H. Tijani. This design consists of three main parts: the speaker, the stack, and the resonator. The speaker is the sound driver which is housed in a sealed chamber connected to the working fluid injector, the BNC adapter for the speaker's power source, and the male connector to the large diameter tube. The large diameter tube connects directly to the stack housing, where the stack resides between two heat exchangers. The heat exchangers interact with the ends of the large diameter tube and a small diameter tube on the other side of the stack housing. The thin tube has a buffer volume at the opposite end, which completes the resonator. Below is a rough sketch that illustrates some of the dimensions and locations of each major component. On a side note, the blue TAR chamber in the illustration is described later in this section as the vacuum chamber. (Tijani, p. 50).

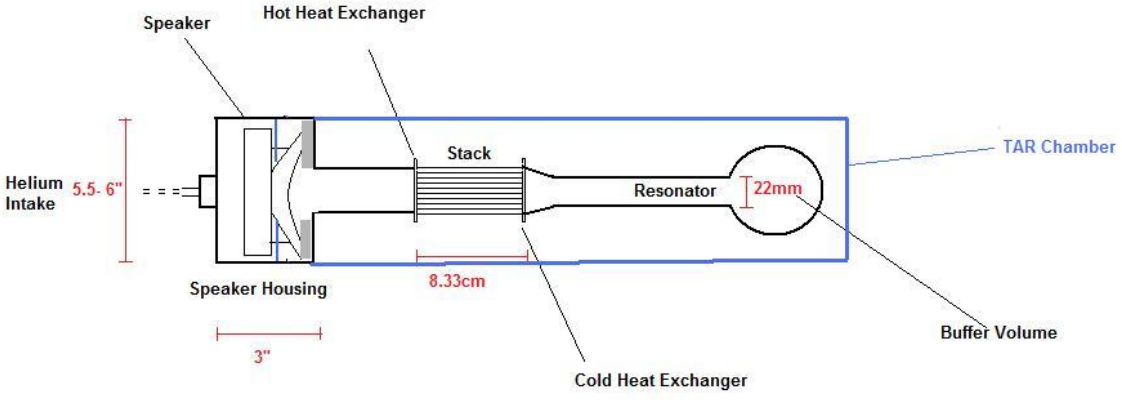

Figure 5 Amateur illustration of the thermoacoustic refrigerator

The previous group chose a stack length of 8.33cm and position of approximately 14.9cm away from the speaker housing according to Tijani's graph relating coefficient of performance to the normalized stack length $L_{SN} = kL_S$. Tijani found optimal normalized stack length around 0.23, which translates L_S into ~8.5cm. For our normalized stack length, we use the resonator length 63 +/- 1 cm and multiply by 4 to determine a wavelength and divide by 2π to get 1/k. Solving for k, we get k = .024 +/- .01, with which we multiply by the stack length 8.33 cm to get our normalized stack length of .207. According to Tijani's graph, this length's COP is just under 1 at approximately 1.35 +/- .05. However, due to the fact that this was not the wavelength used for the cooling experiment, our COP would have been much different (Tijani, p.53).

Before reconstructing the Tijani model of the TAR, we examined possibilities for improving the design by observing what other thermoacoustic engine models are out there. To be more specific, there are variations of each component of the refrigerator which will have different effects.

The first alteration considered was trading out the old resonator for a new tube with a closed end. Having a closed end versus an open buffer volume would trade out a pressure node for a pressure anti-node. A "hard" closed end physically constrains the gas so it has no velocity and is a pressure anti-node; an open pipe will expose the wave to a constant pressure with displacement. A downside to this is that a closed end would actually have more surface area for power absorption of the acoustic wave, so there would be more power loss in the thermoacoustic effect.

With driving power in mind, we also considered replacing the buffer volume with another speaker in order to have a reinforced standing wave. However, this idea boggled our minds as we knew that a large and small diameter tube were needed and would probably have cost us more time to calibrate and coordinate with the other speaker.

Another design option was to try a different geometric pattern or array for the stack. Before even coming up with new designs, it seemed prudent to simply stick with the current, Tijani recommended stack and create an actual effect before changing the design. To determine an effective design for a new stack, equations (1) and (2) must be optimized with regard to the inverse square root of the resonant frequency (higher frequencies will make the depth smaller).

In retrospect, a viable design option was to create a vacuum chamber around the resonator, connected to the bottom of the speaker housing, which would have eliminated the need for a buffer volume. An added benefit would have had very few areas to seal for helium leaks.

Lastly, the materials used to create the resonator were reconsidered. Since copper has a very high thermal conductivity at 400 W/mK (http://www.periodictable.com/Elements/029/data.html) there was no need to exchange either copper tube for another material. The copper wool was reassessed for it heat exchanging capabilities. Ultimately, the ability for the wool to adequately bring heat to or from either part of the stack was limited by the size and geometry of its placement. In other words, the wools had to touch the stack on either side while being able to touch the female copper ends of the large and thin pipes; otherwise the PVC ends of the stack holding would block the heat from

reaching the thermocouples. The wool was shaped to fit as said, but it became apparent that more wool or an entirely other system of heat exchange was needed for the process to work.

Materials

Speaker, Speaker Housing

For the speaker housing, we asked Roger Steele to machine out four holes into the bottom of the PVC drain cap, without drilling through completely. In addition, a second hole that was larger than the other 4 was drilled all the way through the bottom of the cap. This hole was drilled to fit snugly around a male PVC connector that would connect to the copper pipe. We used metal stands as supports to lift the speaker up from the bottom of the drain cap and screwed them in place into holes on the speaker's frame. These metal stands were attached into the four holes using JB weld. Two wires, connected to the positive and negative couples of the speaker, were soldered onto the BNC cable connector that was drilled into the drain cap lid. Teflon tape was placed around the drain cap lid and screwed on very tightly. The PVC connector to the copper pipe was cemented into the large hole drilled into the bottom of the drain cap, and sealed with caulk. This connector was also wrapped with Teflon tape, and screwed on to the copper tube.

After this, we did many pressure tests using helium gas and underwater testing, and found many holes in the drain cap and stack-copper connections. To help remedy this situation, we bought and used liquid latex and applied it around the drain cap trench (along with caulk), the speaker housing-copper tube connector, and on either side of the stack.

The helium tank was fed into the top of the drain cap/speaker housing through a junction with a vacuum to suck the air out of the TAR so as to replace it with helium.

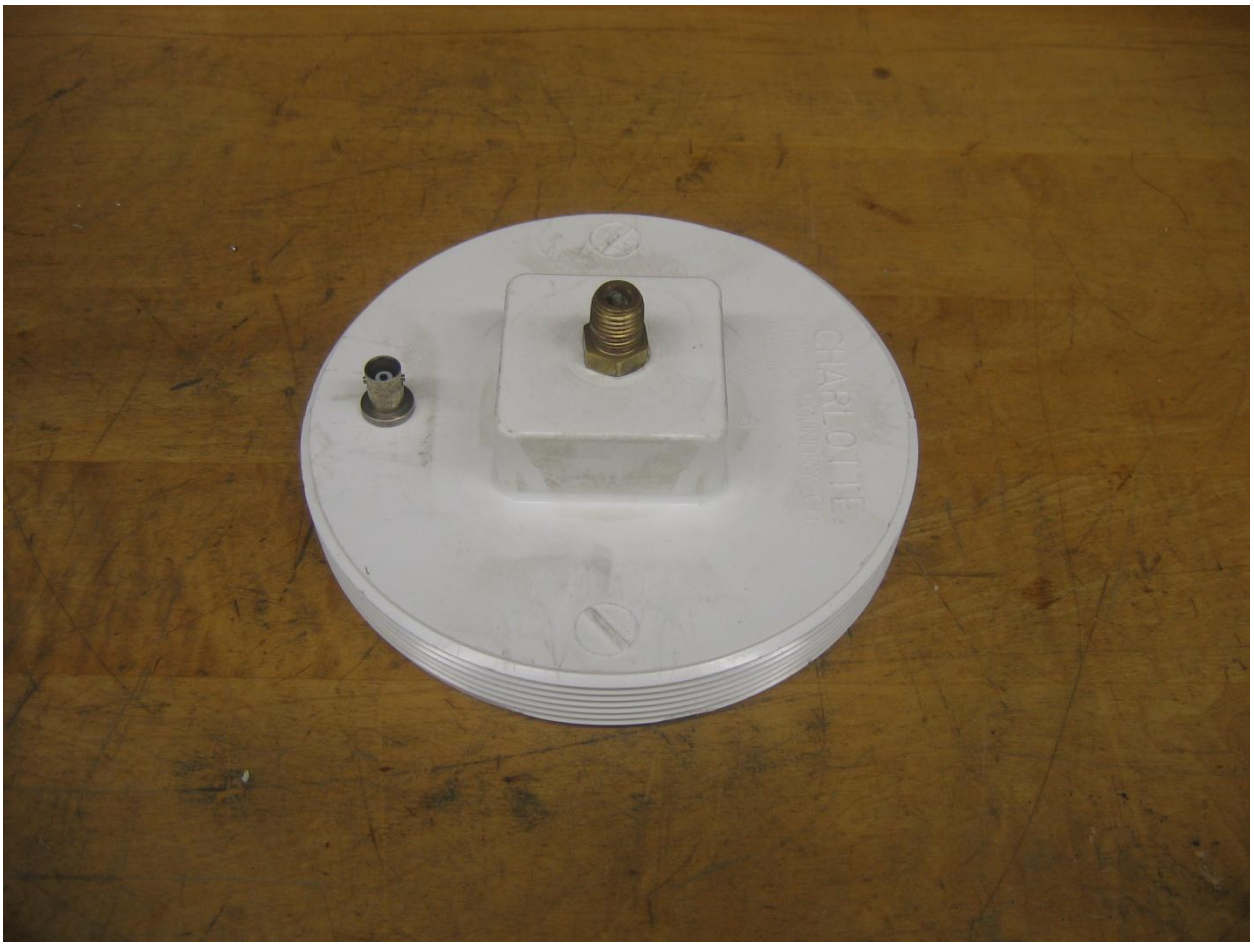

Figure 6 Drain Cap Lid.

For the speaker housing, to make room for a 5” diameter speaker we purchased a 6” diameter PVC drain cap. This drain cap has a screw-on lid, as shown in Figure 6above, which provided easy access into the speaker housing chamber. The grooves along the side were wrapped with Teflon tape in order to insure a sustainable seal, preventing the Helium gas from leaking. We drilled a hole on the top and put in a brass pipe connector which connects to the helium feed, and was the entrance of helium gas into the thermoacoustic refrigerator. On the

side, we drilled another hole and emplaced the power connector for the speaker, which would then connect to the function generator.

Figure 7 the bottom of the drain cap lid.

It proved a bit difficult to tighten the holding, but we managed to solder the connection wires of the speaker directly to the power connector.

Figure 8 The assembled speaker housing.

Figure 9. Close up of the speaker housing.

The speaker housing has a small PVC connector drilled in and placed at the bottom where it would connect to the copper pipe as shown in Figures 8 and 9. We used PVC cement to secure the PVC-PVC connection and JB Weld to secure the PVC-Cu connection, and then followed up on all connection with a sealant layer of Goop and/or epoxy caulk. The smaller PVC connector was approximately 1.5”

Figure 10 shows the speaker used for the set up. Pyle GearX PLG 54.

The speaker itself was a 5” diameter Pyle (250X) with a wattage of 200. Instead of a fragile paper speaker panel, it is made of rubber and plastic for more durability, and is thus capable of creating more power amplitudes of sound waves in the apparatus. The speaker was placed into the speaker housing just above a holding so that the He gas could travel beneath and into the resonator/stack. The speaker itself was fixed in position by using four metal pole which were attached to the housing by JB weld and connected to the power connector on the housing lid.

Figure 11. Bottom view of the same speaker.

The amplifier itself has a max amplifying capacity of 250 watts, so the speaker itself came within safe boundaries, not overloading the system. The speaker was only about $20 and took 5 days shipping overseas from the manufacturer in China.

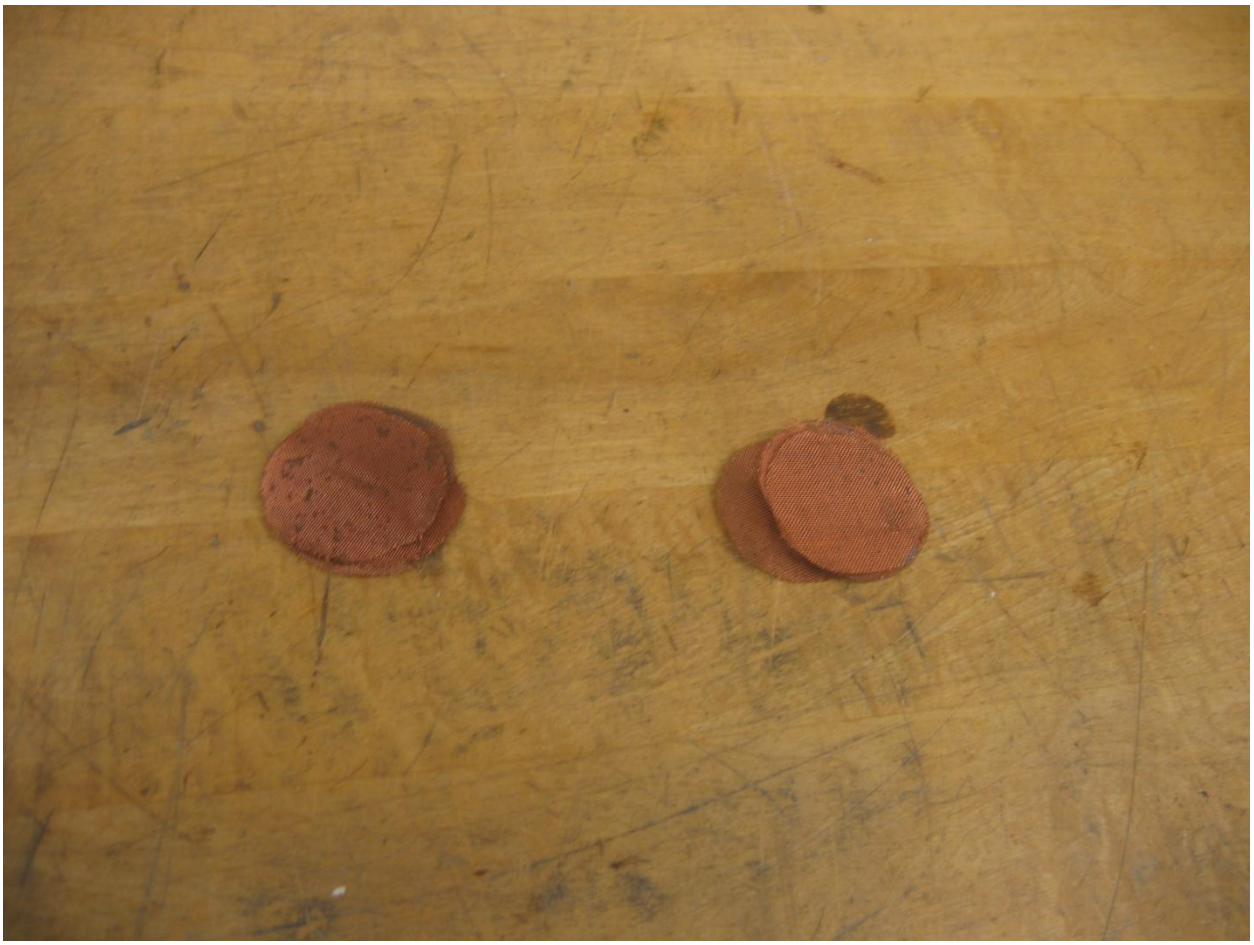

Figure 12 Copper mesh heat exchangers.

The heat exchangers used comprised of two primary components, sections of a copper mesh cut up into 1.5” diameter circles and having 5 placed on either side of the stack. Also, on both the speaker housing and resonator side of the stack, we placed copper wool, which was an even more effective heat exchanger. Although the previous group had a bad experience with the copper meshes we initially used them because the stack housing was longer than the stack and just the copper wool heat exchangers couldn’t reach the copper pipes. It was believed that a combination of the two exchangers would work. Figure 12 shows the copper meshes while Figure 13 shows the copper wool.

Figure 13 Copper wool heat exchanger.

Copper has a very high thermal conductivity, being 400 W/mK at STP, which only succeeded by silver at 430 W/mK. For this reason, it was an excellent choice as a heat exchanger. Having wool of copper creates a large amount of surface area for it to absorb and transfer heat towards the copper pipe which we can then couple our thermal detectors to in order to get temperature measurements.

Stack and Resonator

Overview

Our construction of the apparatus began by disassembling pieces of the old TAR made by the previous group. We recycled their resonator and stack, but not the stack holding. First, we assembled and sealed the PVC components of the stack holding using PVC cement and caulk. The PVC components had to be drilled through in their insides due to unnecessary rings which blocked the ability for us to put the stack in. Each time we applied caulk or any other sealant or adhesive, we usually waited about 4-6 hours for it to completely dry before moving the pieces around and beginning new tasks. After the stack housing was assembled, the stack fit snugly inside it.

Next, the two female copper tube ends were placed together around the middle tube component and soldered on. To seal it, we also applied caulk around the soldered areas. Our copper tube was now complete.

After the stack and copper pipe were assembled, the copper wool was placed inside the resonator tube adjacent to where the stack would connect, and 5 layers of copper mesh were put in to hold the wool and increase the heat exchanging capability. The same process was applied to the copper tube that would connect on the other side of the stack. Teflon tape was then wrapped around the male ends of the PVC stack and then screwed onto the resonator and copper tube parts.

Figure 14. PVC stack housing.

As seen in Figure 14 the stack housing was composed of three parts as well. Two of the parts were male PVC screw-on connectors which were connected to the copper pipe and the resonator. Between these two ends, an external ring of PVC was glued on and sealed. The grooves along the side, as the same as the drain cap lid, were coated with Teflon tape. The diameter of the tube was about 1.5”, just the same as the other PVC and copper connections.

Figure 15 Top view of stack inside the stack housing.

However, on the inside of this pipe, the actual geometric stack was placed. The length of stack was 8.33 cm or 3.3 inches, so our 3.5 inch length stack was a perfect hold for it. Figure 15 shows the stack inside the stack housing which was recycled from the old project. It is a long piece of plastic wrap with thin fishing line strands glued on in many places on melinex wrap and spooled around a wooden peg.

Figure 16 Large diameter copper tube.

The speaker housing was connected to the stack housing PVC by means of a copper pipe shown in Figure 16 constructed from three components, copper being the choice thermally conductive material. The three components were two female ends of a pipe fixture and a small copper ring that fit just within the 1.5” diameter, and then connected by heat and solder. Following that, the copper ring was further sealed using the epoxy caulk.

Figure 17 Resonator with the buffer volume.

The resonator, pictured in Figure 17, from the previous project was recycled and incorporated in ours. It is a long copper pipe which connects on one end to the PVC stack housing and has a glass bulb on the other end to simulate and open end. The copper heat exchangers were placed right at the female end of the thin copper tube.

Problems with Construction

Sealing

The most persistent problem during the construction and testing of the experimental setup was leakage of helium gas. This leakage occurred due to the ineffectiveness of numerous methods of sealant used. At first, we used a pipe sealant called Goop which solidified over a couple hours. Goop failed almost instantly as a helium sealant and adhesive for the separate parts. We then moved on to plumbing caulk for chemically attached pieces of equipment, which worked to a certain extent. There would always be an area that had a small leaking hole that would have to be refilled, which would then have another leak, and so on.

Luckily the most reliable sealant was Teflon tape that was wrapped along the grooves of the screw connectors of pipe attachments and the PVC-PVC and PVC-Copper connections. Our last bid at trying to seal the stack and speaker housing was spraying on liquid latex and letting it dry into a rubbery barrier. Out of the three sealants tried, latex worked the best. However, there were still a few small holes that failed to be sealed. This means that a pressure higher than 1atm could not be sustained without a constant flow of helium gas. This prevented us from testing with pressure greater than 2-2.5atm.

Crookedness, Damage

Applying a chemical adhesive (PVC cement) between the Cu pipe and the speaker housing created a problem with creep. The adhesive was either still drying or simply buckled over time due to the weight of the resonator, causing an angular displacement where the resonator and speaker were no longer in parallel alignment. In addition, at one point our refrigerator fell off the table and caused damage to the inside JB weld hold on the speaker. The speaker had to be reattached to the bottom of the housing, and with irregularities in the now

deformed base of the housing chamber (as the old JB weld was still in the holes in bottom of the chamber), the speaker was slightly crooked. Combining both angular errors could have lead to a significant detrimental effect on the ability of the thermoacoustic refrigerator to function correctly.

Soldering

One minor problem which we encountered was connecting the pieces of the Cu pipe together, namely the two female Cu screw connectors and the middle ring. Since glue and other chemical seals and adhesives were inadequate, we would end up using solder to “weld” the 3 pieces together, and then we applied another layer of sealant (caulk, latex) around the solder.

Experiments

The next step in the project was to test the constructed apparatus. Because of the problems with helium leaks and other issues, there was no clear distinction between the "construction" and "experimental" stage. As some experiments were being done, the apparatus was modified (i.e. sealing leaks, modifying heat exchangers etc.). There are three subsections in the "Experiments section". The "Measurements" section details the work done to set up the experiment and the measurement tools (both hardware and software) used. As explained above, the nature of the project was such that experiments were modified based on previous results. As such, "Experimental procedure" and "results" are combined into the second subsection. The last subsection, "Analysis" explains and interprets the results obtained.

Measurements

Temperature: Thermocouples

The primary measurement for a thermoacoustic engine is the temperature. The use of thermocouples was considered to be the best instrument for the experiment. Two thermocouple type K's were attached to the stack housing on the hot and cold heat exchanger sides. A third end was kept as a measure for the room's air temperature. The other ends of the thermocouples went into a National Instruments USB-9162 Data Acquisition Unit.

Figure 18 Type K thermocouples along with a NI hardware was used to measure temperature across the stack.

Thermocouples work because the junction between two dissimilar metals produces a voltage that is a function of temperature. This junction is formed when the metals touch each other on one end. Type K thermocouples have chromel and alumel wires. For greatest accuracy, the two metals were spot welded at the smallest point. To attach it to the copper stack housing, the surface was first electrically insulated with a dab of General Electric #7031 Varnish. The thermocouples were then attached with a combination of GE varnish, Goop, and super glue shown in Figure 19.

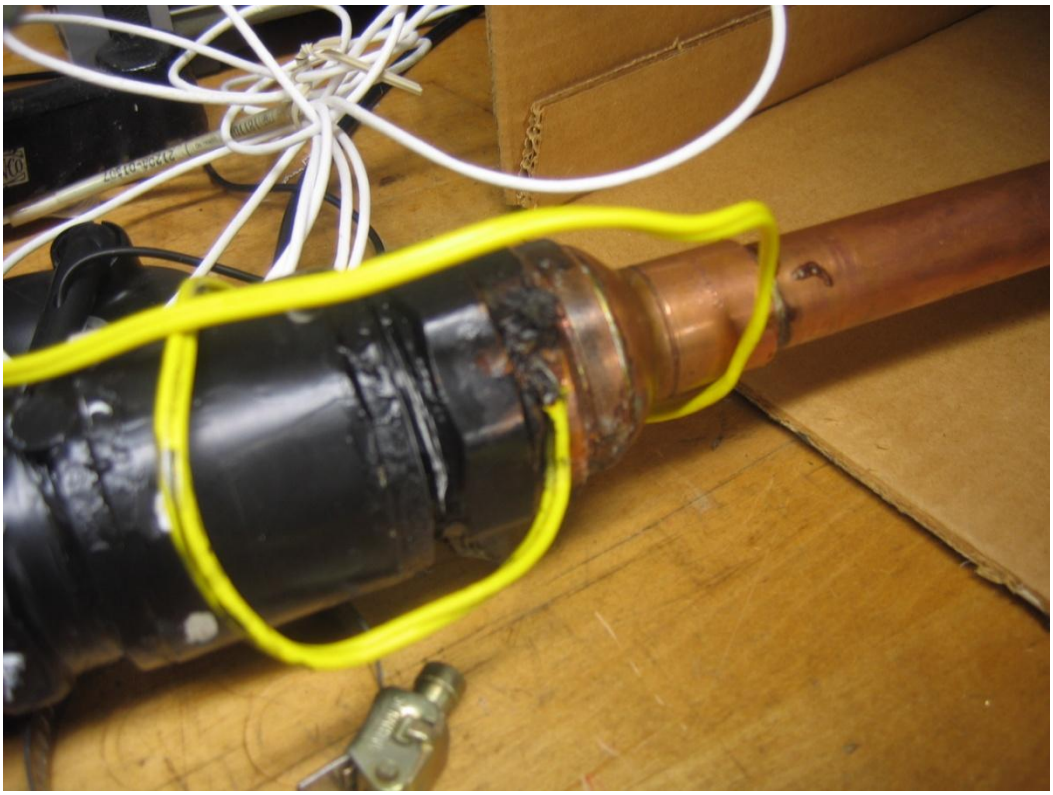

Figure 19 Shows thermocouples attached to the Cold Heat Exchanger side

The computer used National Instruments Labview software to analyze the voltage produced by the thermocouples and convert it into temperature. The virtual instrument was

set up to monitor the temperature and record it to an excel sheet on command. The next section describes how the virtual instrument was set up.

Virtual Instrument: Thermometer

First, a "for loop" was created with a controllable time delay. DAQ assistant was set up to measure temperature from a thermocouple type K. The output signal was split to show the 4 different temperatures. This output was fed into a block array along with a 5^{th} parameter of "elapsed time". It wasn't always necessary to record the temperatures to an excel sheet so the commands to write were included in a true/false loop. The array was fed into a "write to spreadsheet" with the Boolean being true when the "record" button was pushed on the front panel. The file path would be determined each time in the front panel. The column headings were also assigned in the Virtual Instruments block diagram. Figure 20 shows the block diagram of the temperature VI. There were also numerical and graphical displays of the temperature on the front panel. Figure 21 shows the front panel of the VI.

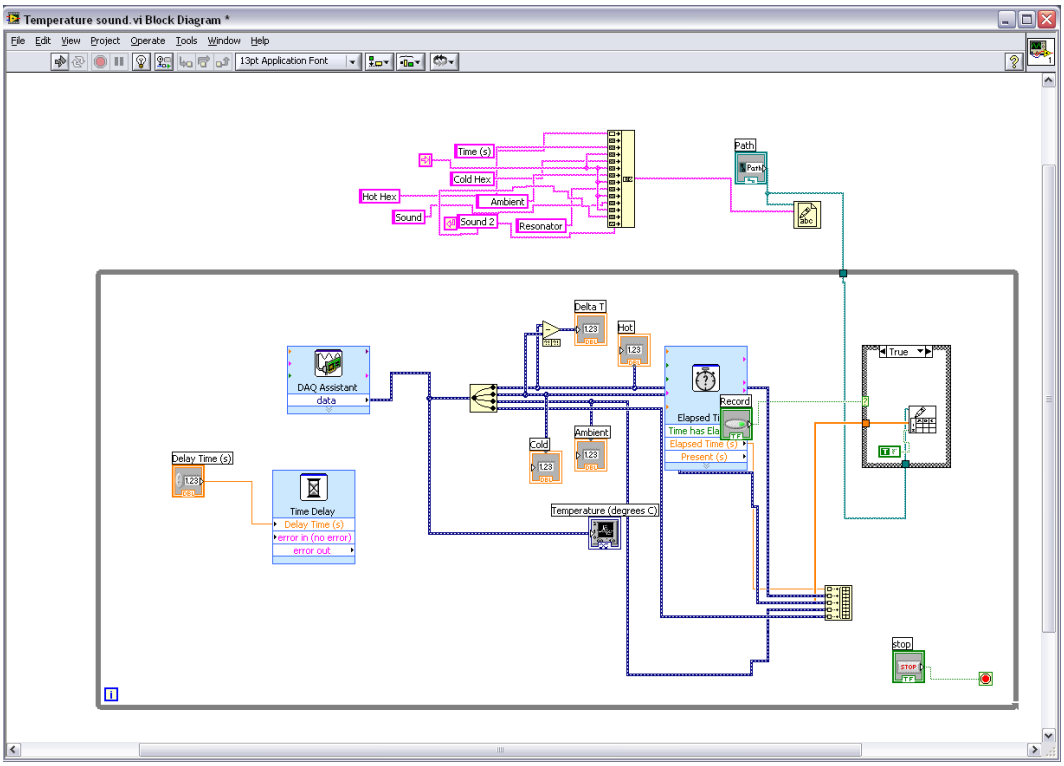

Figure 20 Block diagram of the temperature measuring virtual instrument.

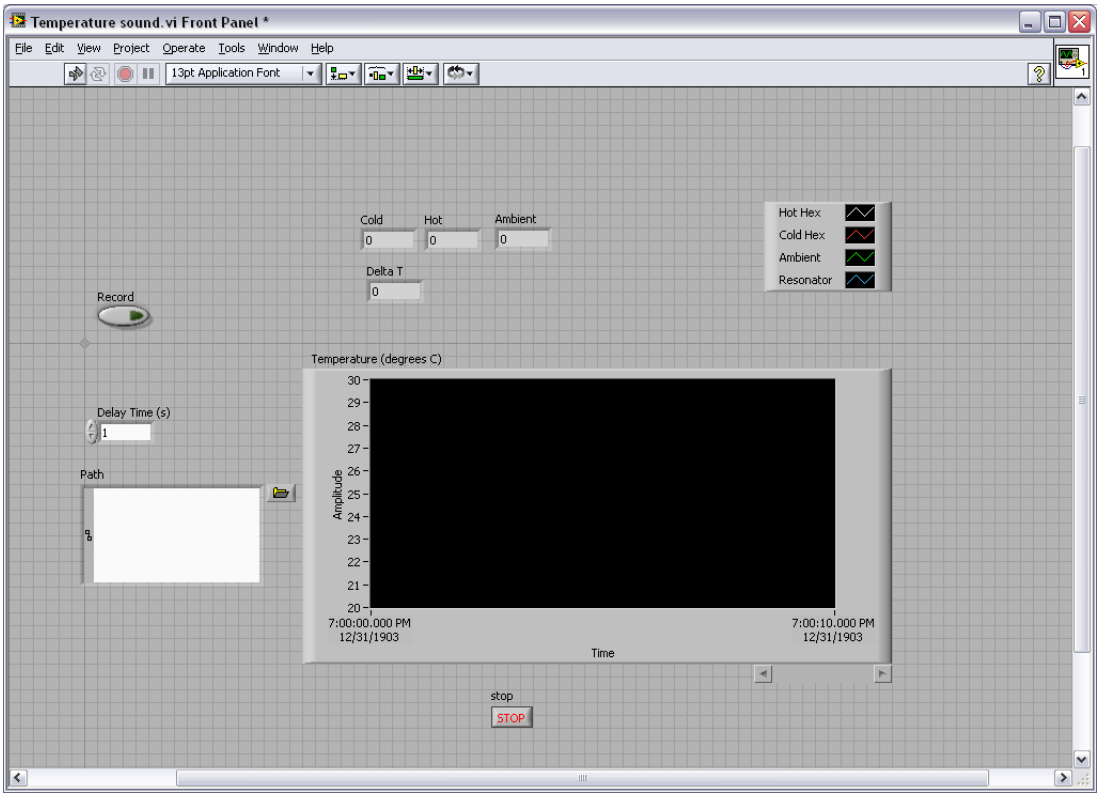

Figure 21 Front panel of the temperature measurement set up.

Acoustics:

In order to achieve a thermoacoustic effect, a standing wave must be created inside the resonator and stack. The standing wave was created by the speaker powered by an amplifier and a wave generator. The main purpose of the measurements was to find the correct resonance frequency for the given set up. The correct frequency was determined by sweeping through a range of frequencies and choosing the one with the highest amplitude. Labview VI's were created to communicate with the wave generator in order to process and record the signals from the microphone.

The standing wave in this set up would have a pressure anti-node at the speaker surface and a pressure node at the open end simulated by the buffer volume. The purpose of

resonance testing was to determine the frequency that would create the standing wave and sandwich the stack between a pressure antinode and node (Tijani, 53).

A Kronhite Model 5920 Arbitrary/Function wave generator was used to vary the frequency of the speaker and a RadioShack 250A PA amplifier was used for power as shown by Figure 22. A Plantronics microphone was used to measure the effect of frequencies. The microphone was placed very close to the resonator and surrounded with wool so as to block other vibrations.

Figure 22 Shows the Radioshack Amplifier stacked on top of the Kronhite Wave Generator

Since the wave generator did not have a knob to sweep through, frequencies would either have to be stepped manually or programmed. A VI was made to communicate with the wave generator using a GPIB connection. The wave generator was capable of accepting ASCII commands to change the frequencies or amplitude. Unfortunately, the VI was not able to have a (virtual) knob that could send continuous commands to the generator. Moreover, sweeping the frequencies that fast would not provide the correct data since every frequency would need a certain amount of time to settle. Frequencies were thus varied manually.

Since a resonant frequency would create the highest amplitude, the challenge was to measure the amplitude or strength of each frequency. The signal received by the microphone would contain a mix of frequencies and amplitudes. A conventional graph of amplitude vs. time would be very impractical for determining which frequency is dominant and by how much. A frequency domain data would display exactly that and would be much more suitable for this situation. The time domain data can be converted to a frequency domain data by a process called the “Fourier Transform”. The Fourier transform itself is fairly complicated can be performed by any signal processing software.

Converting the voltage output from the microphone into accessible usable data was a challenging task. A program known as Spectrum Laboratory was tested first. The program performed a Fourier transform and displayed nice peaks over a range of frequencies but was tough to work with. It was especially hard to write the data to an excel file without receiving an overwhelming amount of data. Once the data was in the excel file, finding the peak amplitude was a formidable task as well. To observe a peak, one would have to average the plethora of

data points provided by the program and graph it. This proved to be inefficient. Since the program was unfamiliar anyway, Labview was chosen for the task instead.

A virtual instrument was created in Labview that could perform resonance testing. Many days were spent trying to create a VI from scratch, or modifying a VI available on the internet, to suit this purpose. It was later discovered that Labview had a built-in subVI that could convert sound voltage input into data. This subVI, combined with another subVi that would take "Fast Fourier Transform" of the data, was used to create the final VI that can be seen in Figure 23.

Many parameters could be adjusted within the VI to augment our measurements. The sampling frequency determines the range of frequencies that could be accurately measured without the effects of aliasing. The frequencies of interested in the experiment were less than 4 kHz; so, the sampling frequency was lowered to its minimum level of 8 kHz. The time resolution Δt in the time domain was inversely proportional to the frequency resolution Δf on the frequency scale. This parameter was adjusted depending on the frequency resolution needed. The next section details the Labview VI for resonance as seen in Figure 23.

Virtual Instrument: Resonance

Sound was first recorded by the "acquire sound" subVI. This could be configured for sampling rate (which was set to 8 kHz) and duration Δt as shown in Figure 24 . The data was then sent to "spectral measurements" which took the Fast Fourier Transform of the signal. This VI could be configured depending on the type of signal. For these experiments, "power spectrum" with a "Hanning" window function was chosen, as shown in Figure 25. Finally, the data was recorded to an excel file. The front panel also displayed the spectrum as shown in Figure 26.

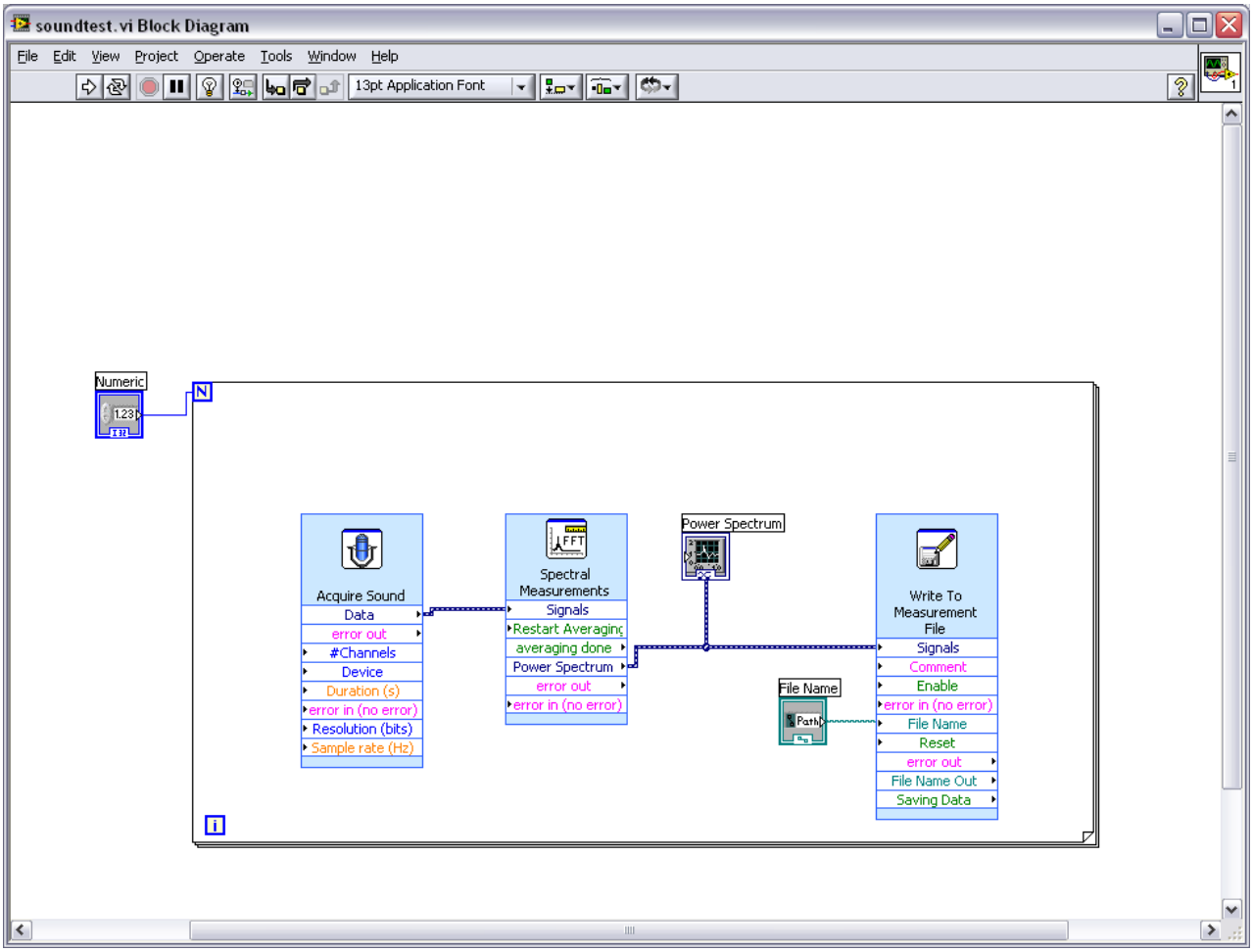

Figure 23 Block Diagram of the resonance measurement VI.

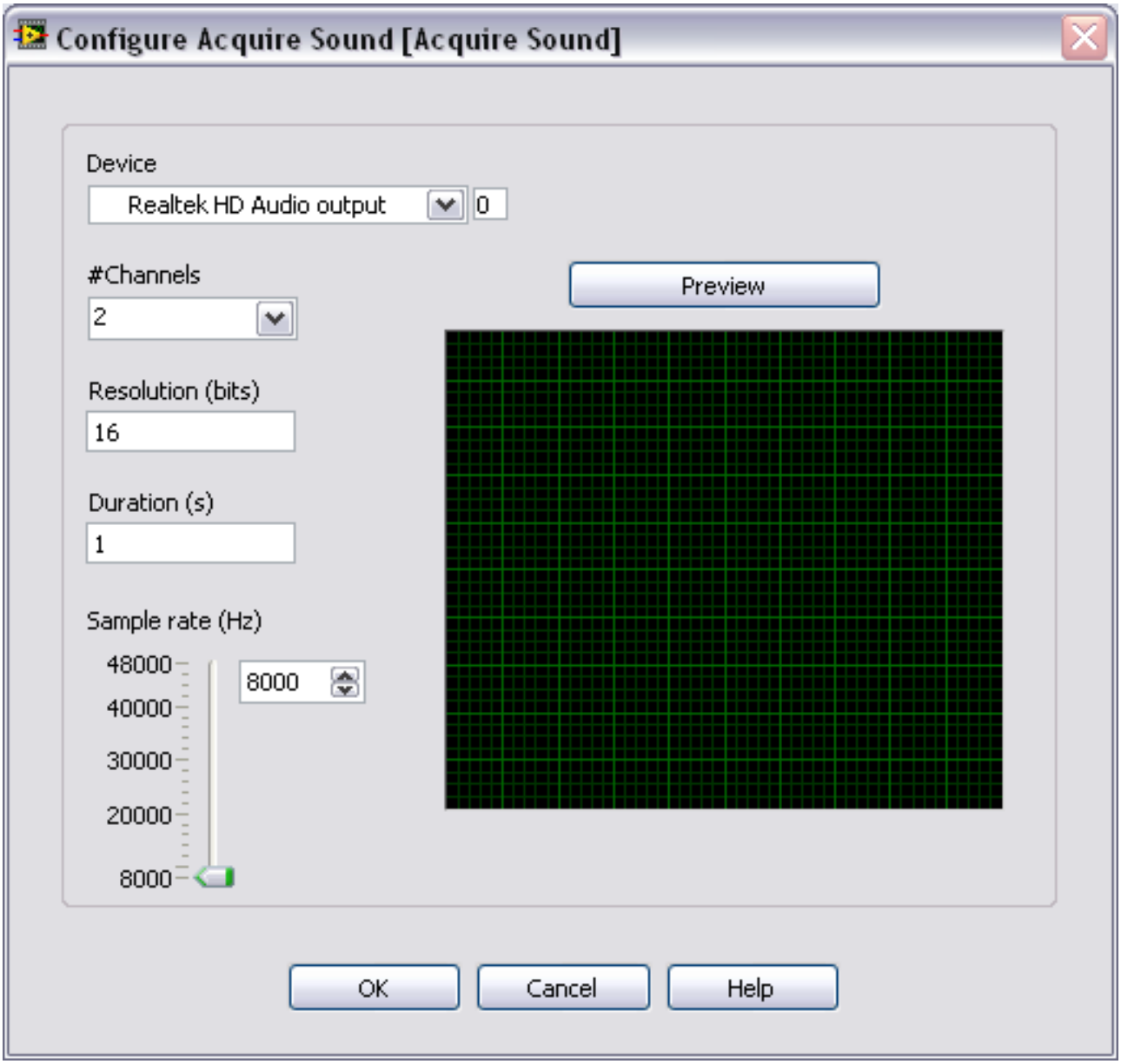

Figure 24 Settings for the "Acquire Sound" Sub VI.

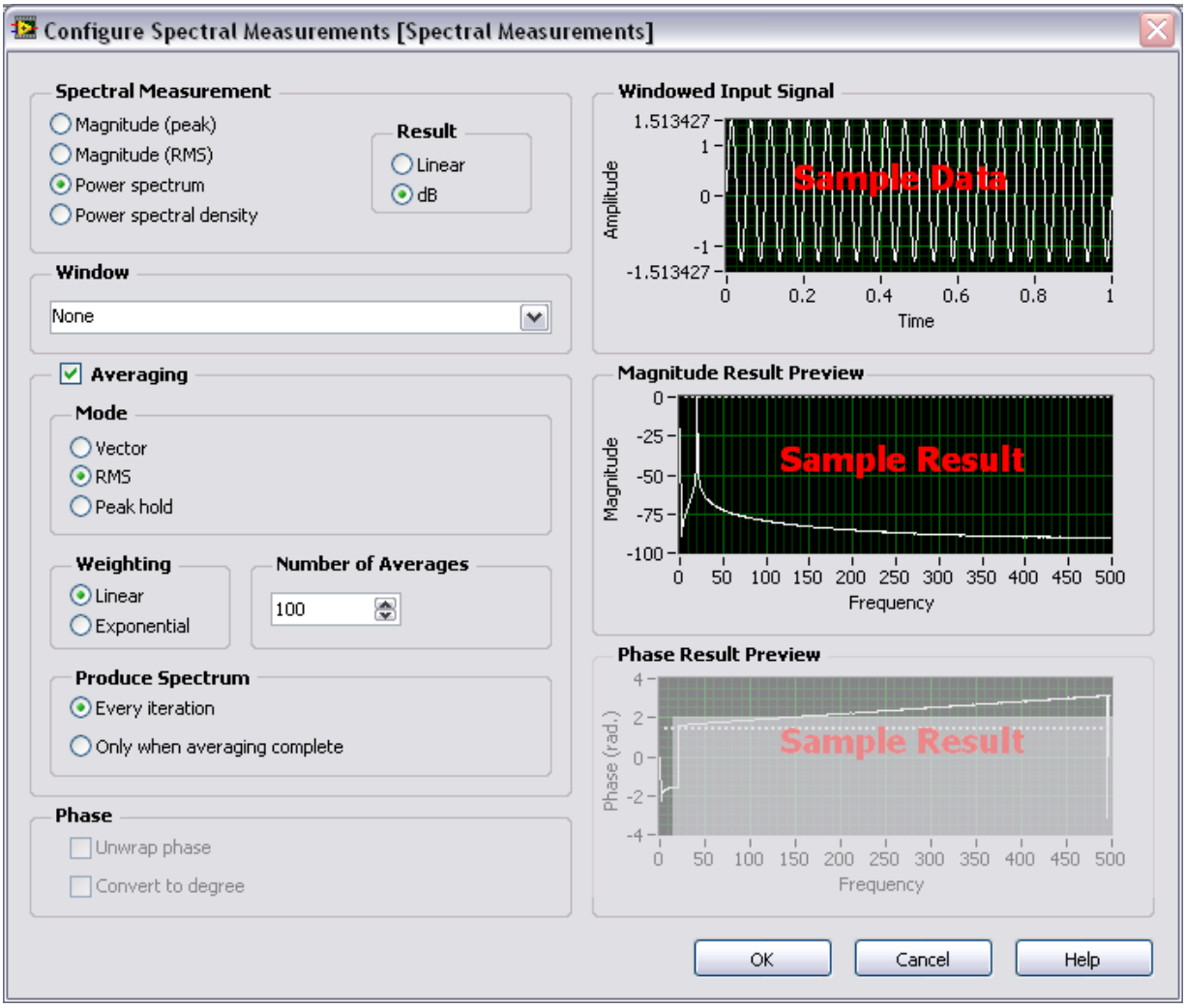

Figure 25 Settings for the "Spectral Measurements" sub VI.

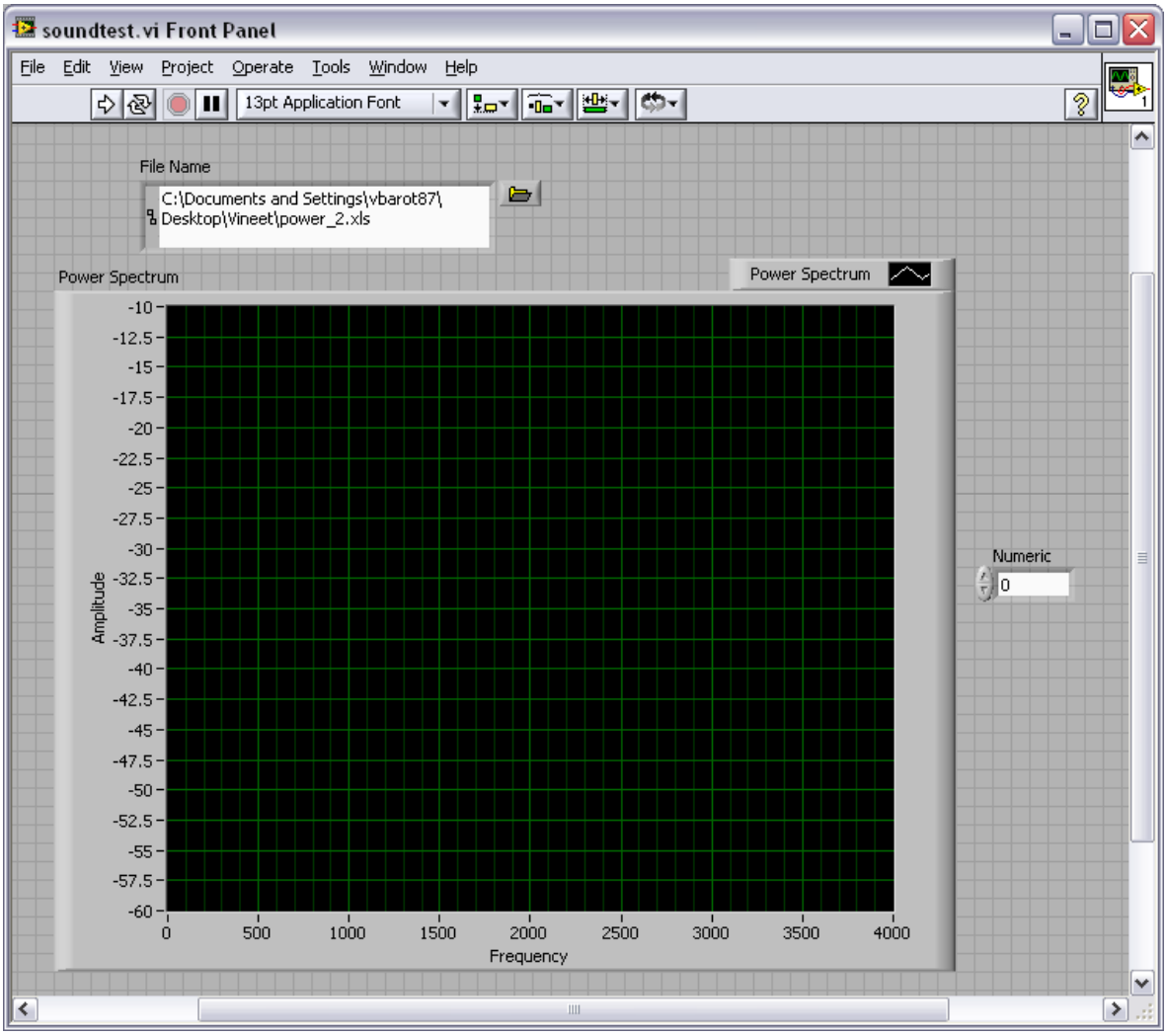

Figure 26 Front Panel of the resonance test VI

A combination of the wave generator and the resonance VI could now be used to obtain resonance data. A sample experiment would go as follows: measurements were first made at large intervals, such as 100, 250, 500 and 1000 Hz at a resolution of 10 Hz. The frequencies with the two highest amplitudes were taken as the range for the next set of measurements. The next set, for our example, would be to measure at 100, 125, 150 etc. at a resolution of 1 Hz. As expected, in almost all measurements, the driving frequency and the peak frequency were the same. The process was a little tedious and a more efficient VI would assemble a list of all

maximum frequencies and their amplitudes. Nonetheless, this method was effective in getting the resonance. Since the resonance frequency is constant for every gas for a given temperature, only two resonances (for air and helium) were needed to be measured.

Experimental Procedure and Results:

Overview:

There are three distinct steps for conducting the experiment on a table top thermoacoustic refrigerator.

1. Inject the working fluid (helium) in the refrigerator
2. Conduct resonance testing to find the usable standing wave frequency.
3. Measure the temperature change of the heat exchangers at the resonant frequency.

Gas Mixing

To facilitate in higher pressure gas mixing, a T junction was created with copper tubes show by Figure 27 below. Two different valves, one connected to a pressurized helium tank and the other to a vacuum pump were used to fill the apparatus with helium. The helium tank had a pressure gage and the pressures mentioned in the report are in absolute atms based on the readings from this gage which had an uncertainty of .1 atms. Since the refrigerator was not necessarily prepared for a full hard vacuum alternating between vacuum and helium feeds would eventually fill it with helium. For the experiments, the procedure went as follows: 1. Turn on vacuum and leave it for 10 minutes 2. Turn on Helium and leave it for 10 minutes 3. Repeat. Because Helium escapes easily, the helium feed valve and tank were left on throughout the experiment the idea being that any leaks would be forced leaks and would be promptly replaced by more helium. As will be seen later, this wasn't always the case.

Figure 27 Shows the valves used for gas mixing.

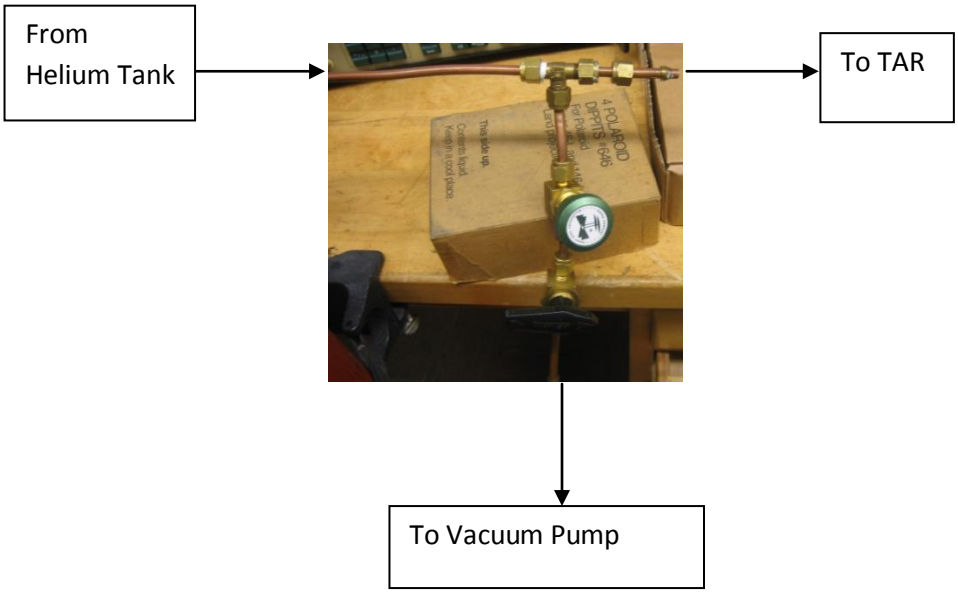

Resonance Testing

The first step was to determine the resonance frequency of the thermoacoustic refrigerator. As described previously, the testing was first taken with large steps in frequencies, and the steps were eventually lowered to "zone in" on a particular frequency. The refrigerator was then tested at the determined frequency for helium at different pressures. The spectrum analysis of various frequencies (in air and helium) was conducted first at a constant 1 atm pressure. After compiling a list of amplitudes for different driving frequencies, the resonance for the particular system was determined.

Air

Although air was not the desired working fluid for the refrigerator, resonance testing was first done on this as a practice. Frequencies of 100, 200, 300, 500, 1000 Hz at a resolution of 1 Hz. Figure 28 below shows the result for 200 Hz.

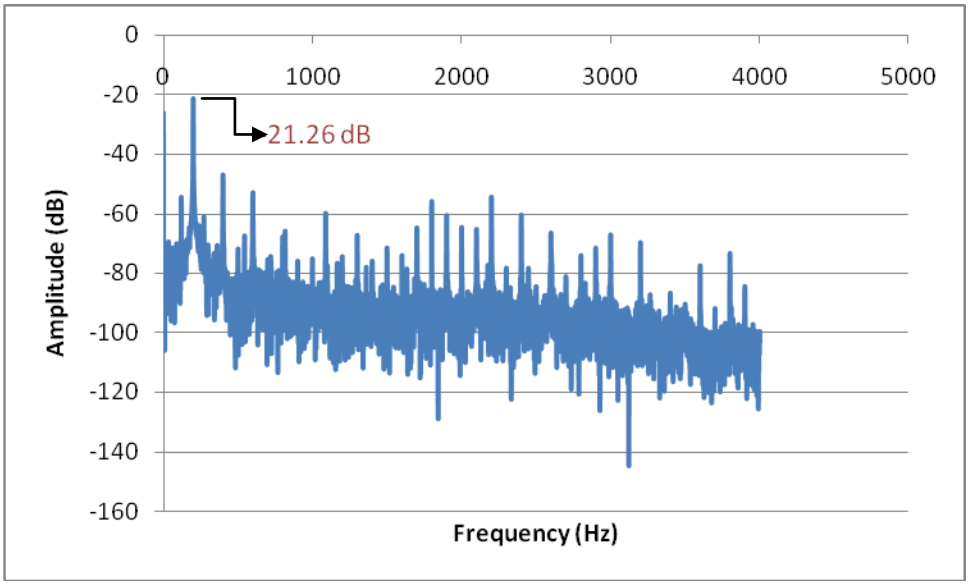

Figure 28 shows amplitude vs. frequency for Air at 1 atm at a driving frequency of 200 Hz.

Figure 28 shows a lot of different peaks but the most prevalent one was at the driving frequency of 200 Hz. Similar graphs were obtained for the other frequencies. The largest amplitudes were of 100 Hz and 200 Hz. Since 200 Hz had larger amplitude, the resonance was likely closer to 200 than 100 Hz. Frequencies between 150 and 200 were swept at 10 Hz intervals with a resolution of 0.1 Hz. In order to analyze the spectrum more fully, the amplitude for each frequency was recorded and tabulated. For example, in Figure 28 above, the entry would be freq=200 Hz and Amplitude=-21.26 dB. This process of "zoning in" on the resonance frequency was continued until a satisfactory set of data of amplitude vs. frequency was collected. Figure 29 below shows the graph of Amplitude vs. Frequency for air at 1 atm. Figure 30 shows a narrower range between 174 and 184 Hz for a closer look at the resonant frequency. It also shows the driving vs. measured frequency to display the fact that they closely match.

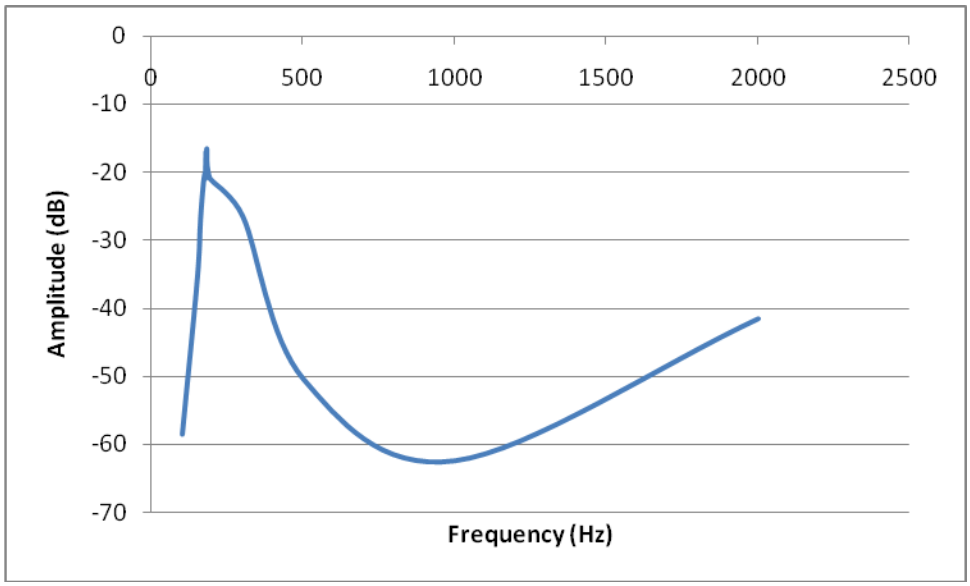

Figure 29 Amplitude vs. Frequency of Air at 1 atm. This figure shows all the tested frequencies.

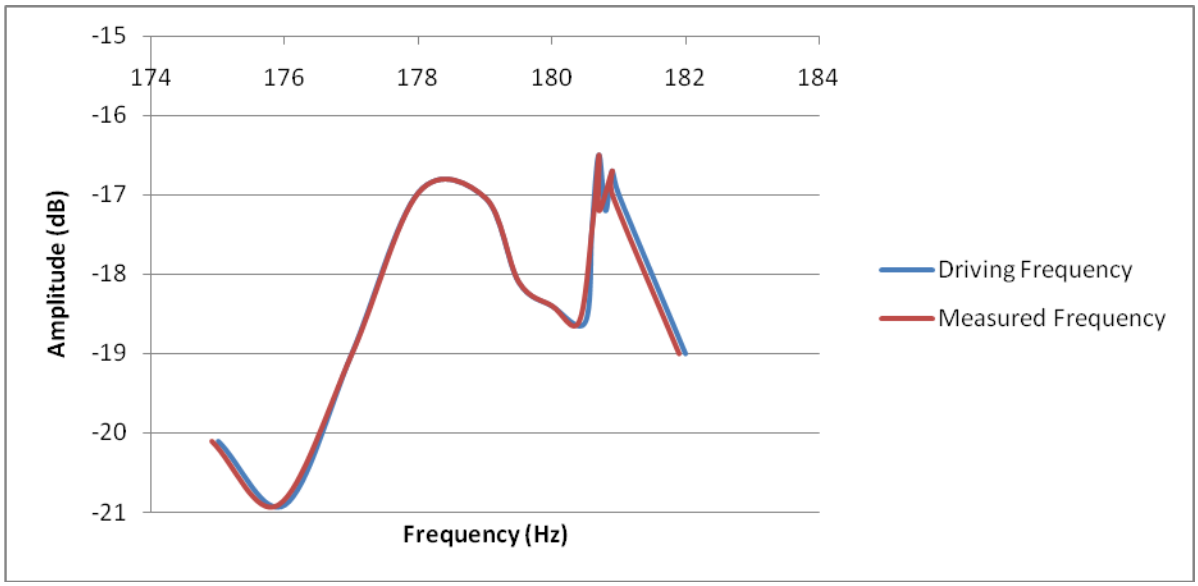

Figure 30 shows a narrower range of amplitude vs. frequency for air at 1 atm.

About the graphs:

It is important to note that the graphs shown in Figure 29 and 30 are scatter plots with Microsoft Excel's attempt to fit lines through it. While it makes visualizing the data easier, it can

lead the reader astray when analyzing between points. The analysis was done carefully and only considered the actual points that were measured.

Helium

The procedure for helium was the same as for air. Figure 31 below shows the graph for Helium at driving frequency of 700 Hz at 1 atm. Many such data points were collected and Figure 32 below shows the assembled graph for the different frequencies.

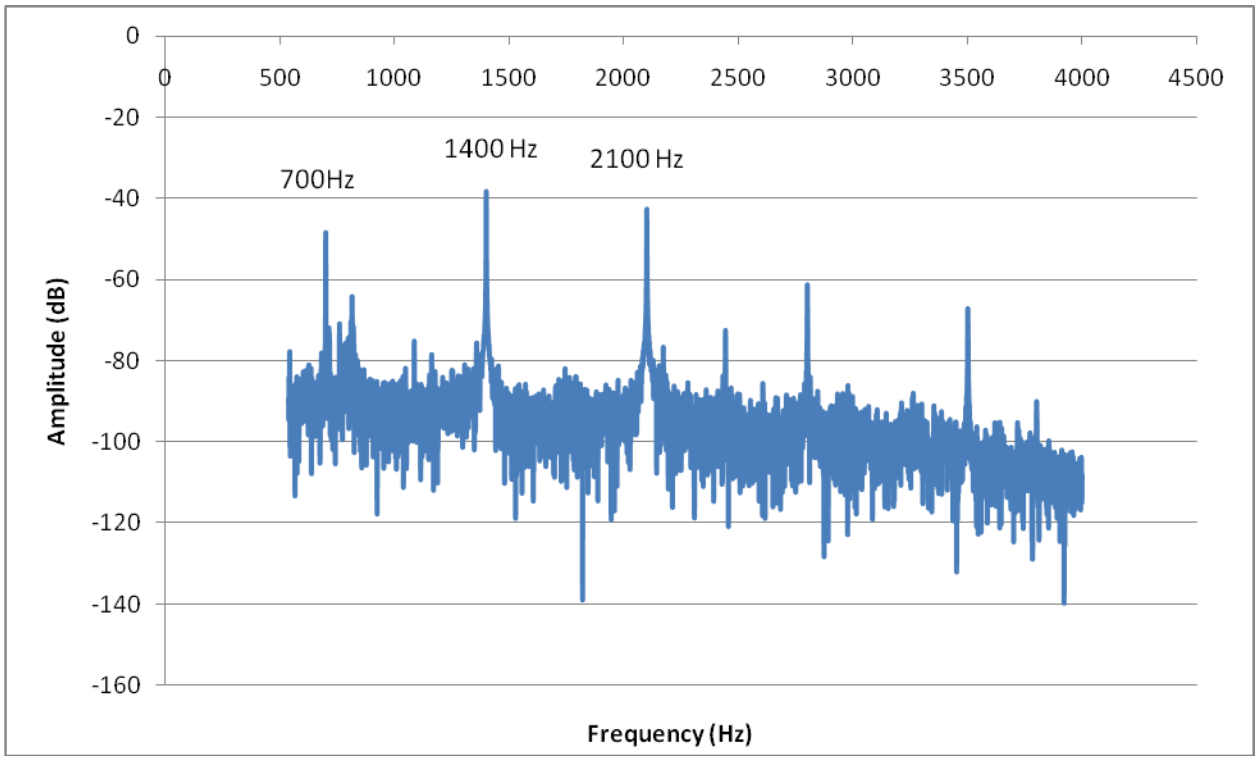

Figure 31 The frequency spectrum for Helium at 1 atm for the frequency of 700 Hz.

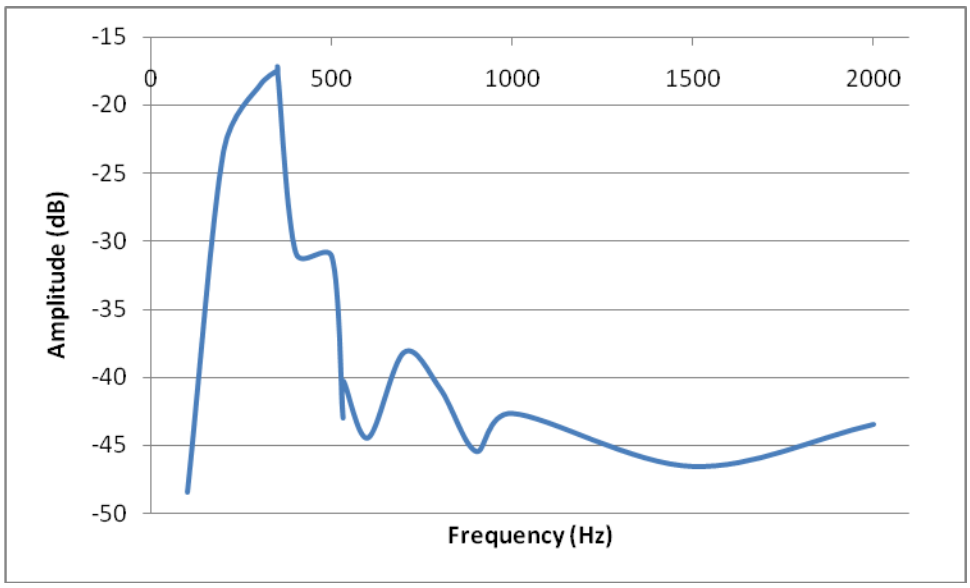

Figure 32 shows the assembled data of amplitude vs. frequency for helium at 1 atm.

Temperature

Temperature testing was conducted at the resonance frequency of air and helium at different pressures. Ideally, the experiments would have yielded a lot of data but only a couple of full experiments were recorded. Not all of those testing data were recorded but the effects were observed through the graphical display on the front panel of the Labview software. The data that was recorded is displayed for analysis.

The first set of experiments was conducted when the heat exchangers consisted of a combination of copper wool and copper meshes. Figure 33 below shows the temperature at 1 atm of air with a speaker driving frequency of 100 Hz.

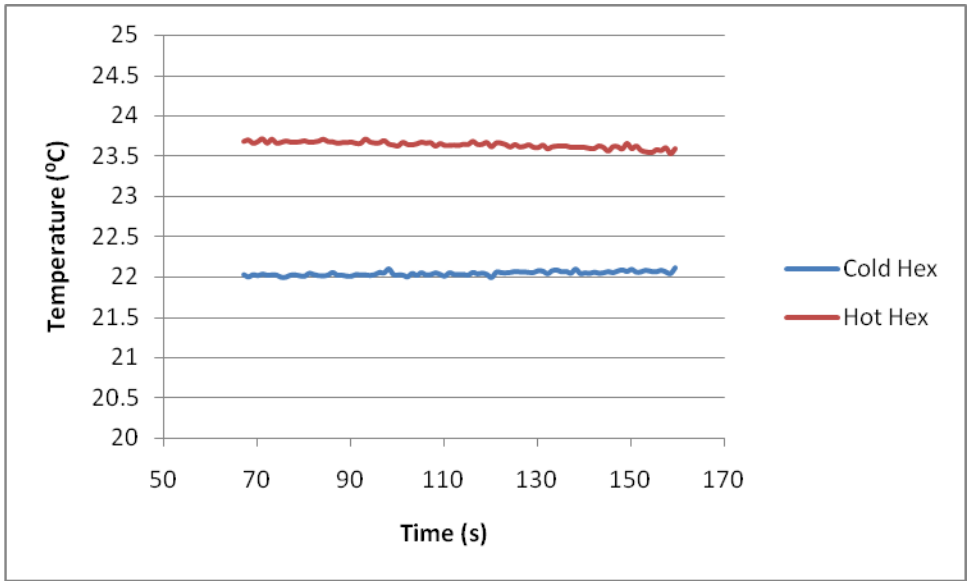

Figure 33 Temperature data for air at 1 atm and frequency of 100Hz.

Many of the other experiments at different pressures and frequencies for both air and helium were observed to have similar graphs. None of them showed any overall change in temperature.

The second set of experiments was done using only the copper wool as the heat exchangers. Figure 34 below shows the temperature data taken after the copper meshes were removed. This is the graph of temperature vs. time for helium at 2.5 atm. No other experiments were conducted after the copper meshes were removed because of time constraints and because the speaker stopped working. The time constrains came from the second set of experiments. Because of the sealed nature of the apparatus, taking it apart and reconstructing it takes a fair amount of time. Figure 35 shows the same graph but with the ambient included. Two different graphs are displayed because the thermocouple that was measuring the ambient

temperature was compromised (i.e. it was moved around) after a short time into the experiment.

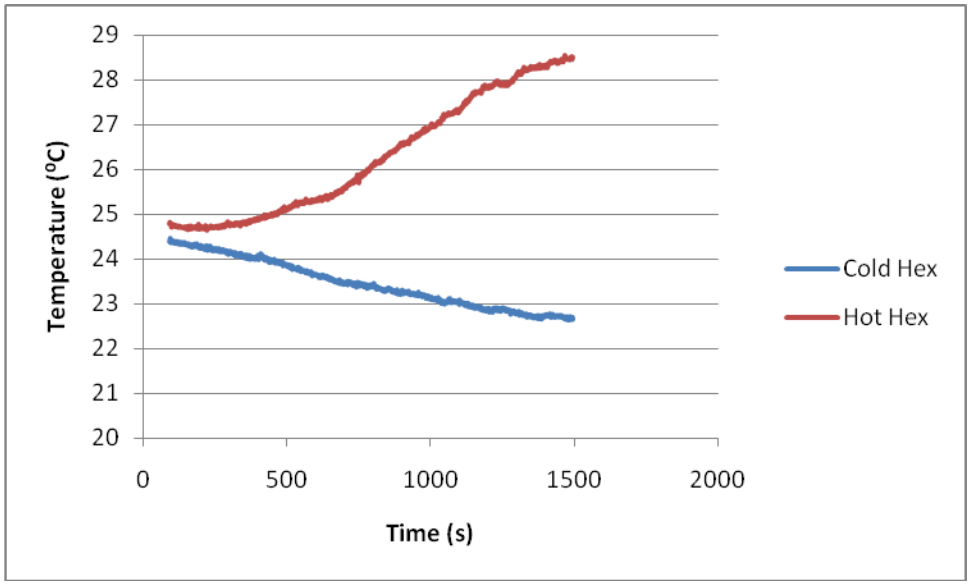

Figure 34 Temperature data for Helium at 2.5 atm and resonant frequency

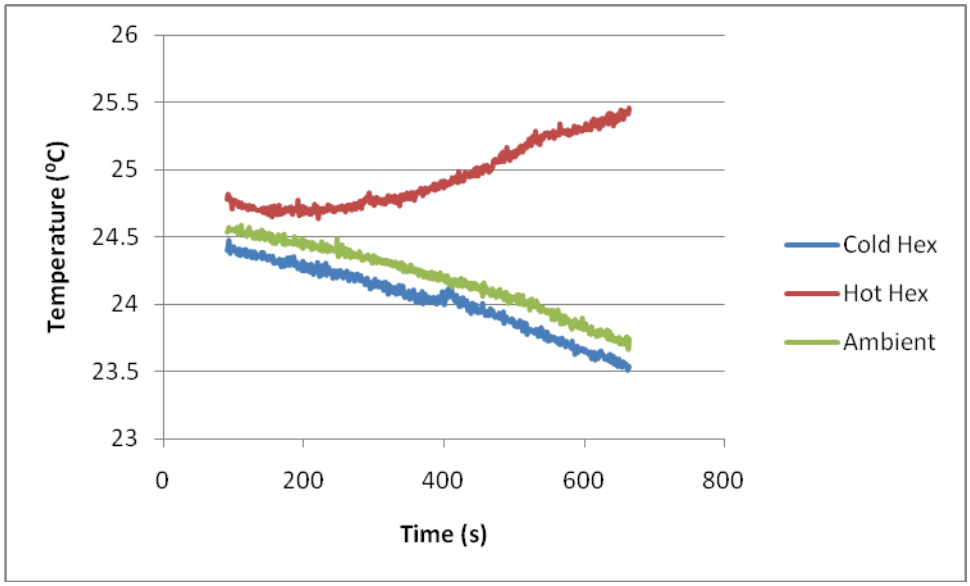

Figure 35 Temperature vs. Time for Helium at 2.5 atm and resonant frequency with ambient temperature.

Analysis

The frequency spectrums for different driving frequencies were used to compile a list of amplitude vs. frequency graphs for both air and helium. In this section, the data is analyzed and the resonant frequency is determined. The impurities and inconsistencies of the frequency data are also explored. Although there were relatively fewer temperature recordings, there was enough observational data to be explained in this section.

Resonance

Figure 28 and Figure 31 show the frequency spectrums in air and helium at different frequencies. Figure 28 has many peaks but the peak for the driving frequency of 200 Hz is the highest. The other peaks are all multiples or harmonics of the frequency. In some cases the harmonic has greater amplitude than the driving frequency itself such as Figure 31. Since multiples of the base resonant frequency is also a resonant frequency, the amplitude from the harmonics was recorded for the overall graph of Figure 32.

Even with the explanation of harmonics, there are still many others, albeit smaller, peaks present in the frequency data. In an ideal condition, such as blowing into one smooth pipe, the amplitudes would be highest at the harmonics and zero everywhere else. This apparatus was not ideal because of its many small parts and complex geometry. Every part, from the valves connected to the gas cylinders to the buffer volume, had its own resonance or natural frequency. Although the microphone was placed at the center of the resonator, these different natural frequencies corresponded to the noisy signal received by the microphone.

Figure 30 shows that the highest amplitude was achieved by a driving frequency of 180.7 Hz. There is another sharp peak at 180.9 Hz. Another interesting anomaly are the peaks

around 178 Hz. While the discrepancy of 0.2 Hz can be explained by a small error, the other peaks around 178 Hz indicates that the uncertainty in determining the resonance frequency is about ± 2 Hz. Thus, the final resonance frequency for air was determined to be 180 ± 2 Hz.

The frequency vs. amplitude data for helium at a pressure of 1 atm is given in Figure 32. Using the same procedure and logic that was used for air, the resonance frequency for helium was determined to be 349 ± 2 Hz. This is vastly different from the expected frequency of around 409 Hz for which the apparatus was originally designed. Since the length of the apparatus is a fixed λ/4, the measured frequency could be used to calculate a length. If this backwards calculation is correct, then the resonance testing was successful. Table 1 shows that the calculated length is much closer to the actual length with a frequency of 409 Hz. Because the calculations were based on the sound velocity and the measured frequency, this implies that one of the two is incorrect. There had been very few problems encountered with the resonance testing and there was clearly a peak around 350 Hz in Figure 32. But the speed of sound used for the calculation assumes that the working fluid is purely helium. Because the system had many leaks, it is possible that the speed of sound was in fact different .

Table 1 shows the calculated length

	Temperature	c	Frequency	Wavelength	Calculated Length	Actual Length
Helium	25	1017	349	2.914910535	0.728727634	0.63
			409	2.487295298	0.621823824	0.63

While a possible reason for this discrepancy is the non-ideal geometries and many different parts used in the construction of the refrigerator. The most likely reason is the lack of

a pure mixture of helium. When helium leaks out, air takes its place and because it has a lower fundamental resonant frequency (180 Hz for this case), a mixture of helium and air would have a resonance frequency in between air and helium, i.e. between 180 Hz and 409 Hz which is exactly what we observed. It is also concluded that since the frequency was much closer to helium than air's, that the fluid inside was mostly helium.

Temperature

As mentioned in the "Materials" section, copper meshes were used along with the copper wools for heat exchangers for the first part of the experiment. This may have had an effect on not seeing a lot of temperature variation. When the copper meshes were removed, only one set of measurements were conducted before the speaker malfunctioned.

To confirm that the refrigerator cools using the thermoacoustic effect , there would have to be a significant temperature difference between the hot and cold heat exchangers. Many tests were done with helium at different pressures with the goal of seeing the thermoacoustic effect. Figure 33 shows no overall variation in temperature throughout the experiment. Although this experiment was not at the resonance frequency, it is close to the kind of results that were observed in a lot of different set ups. Since the temperatures could be viewed on the front panel of the Labview VI, most temperatures were not recorded. Some of the other data that was recorded was, unfortunately, erased. This happened whenever the VI ran on the same file name but the record button was not pushed. At the end of the first set of experiments, no thermoacoustic refrigeration was observed.

It was determined that poor heat exchangers may be a cause of this. In their report, Lingenfelter and LaBounty claim that the copper meshes did not work for their apparatus. Despite their recommendation, the copper meshes were originally used because the stack housing was slightly larger than the stack and the copper wools weren't large enough to directly contact the copper female ends on either side of the stack. Also, the amplitude through the speaker was increased slightly so that its full power could be used.

Figures 34 and 35 show the temperature data of that particular experiment. Figure 34 seems to show some cooling in the cold exchanger while the hot exchanger increased in temperature by about 4 degrees. At first, this was determined to be a possible thermoacoustic effect. Figure 35, however, shows the same data with the ambient temperature included. Only part of the timeline is shown because the ambient thermocouple was touched and moved around to measure the temperature at different parts of the refrigerator which compromised some of its data. Many more ambient data points were, however, were measured and observed. By observing the ambient temperature along with the corresponding temperatures for the hot and cold heat exchangers, it was concluded that there was no thermoacoustic effect. The hot heat exchanger got hotter than usual because of the heating of the speaker. At the end of the experiment the speaker did not function suggesting that the amplifier may have driven it higher than its rated power. The cold heat exchanger got colder because of the drop in ambient temperature.

Possible Mistakes

From the analysis section, it is clear that after many experiments and reconstructions, there was no thermoacoustic effect measured. This was true even though this project used many of the same design aspects and better components than the previous project. The thermoacoustic refrigerator also ran at a higher pressure and with a better speaker. Why did this project not see a thermoacoustic effect while the previous project did?

One of the main causes was the lack of pure helium in the refrigerator. Sealing the apparatus in all its different joints and nooks had been a problem from the very inception of its construction even with the helium feed running during the experiment. This was evidenced by the lower than expected fundamental frequency that was measured. Since the design was based on pure helium and a resonant frequency of around 409 Hz, the stack length was not ideal for an air-helium mix. In other words, the problem wasn't that there was a "wrong" resonance measurement but rather that the placement and length of the stack was optimized for a different environment.

The resonance measurements themselves, while not incorrect, had a fairly high error. This was because of the many different components used and their respective natural frequencies and diameters. The resonance curves for different driving frequencies weren't very clean and neither was the assembled set of data. Ideally, the sound waves would travel only in one direction and without much dissipation. Because of different materials and diameters, and

because the apparatus itself was slightly skewed, this idealization was probably not true. It was also assumed that since the velocity of sound only changes with temperature that resonance measured at 1 atm of helium could be applied at 2.5 atm of helium. But, because the working fluid tended to be a mixture of air and helium, the ratio of the mixture and thus the resonant frequency at 2.5 atms was likely much different than at 1 atm.

In the next section, it is shown that the previous project may not have seen a thermoacoustic effect either. If the previous project did not work, it would have several implications on the outcome of this project. First, many of the components, most importantly the stack, were recycled. If the previous project did not work the components may be a big reason for that. A reconstruction with the same parts would naturally have a very low chance of working. Secondly, it may also suggest that table top thermoacoustic refrigerators of this design and type may not work very well in general.

There are many other minor reasons for why the experiments yielded in a lack of a thermoacoustic effect. One mistake was not being able to gather enough experimental data to have more conclusive results. Another improvement would be to let each experiment run longer and to measure the resonant frequency after a certain period of time to correct the frequency.

Possible mistakes of the previous project

The previous section outlined possible reasons of why the current refrigerator did not work. But it is also likely that the effect observed by the previous project was incorrect.

In terms of experiments, the two projects went along a very similar path. There was no effect seen in the first set of experiments. Once the copper meshes were removed, a temperature difference was measured across the stack but the speaker blew after that. The only difference being that previous group ran their experiment for a longer period of time and observed a larger temperature difference. But, their temperature measurements were done by using a quartz thermometer that simply displayed a temperature *difference* (LaBounty et al., p. 55-56). Looking at Figure 34, one can see that if only the temperature difference is calculated, then it would be concluded (falsely in our case) that a thermoacoustic effect was present. To address this issue, LaBounty and Lingenfelter measured the ambient temperature at every hour (LaBounty et al., p. 56-57). As seen from Figure 35, the ambient temperature of the room varied within minutes and thus an hour might have been too long of a period for ambient measurements. They also tried to measure the resistance heating of the speaker in a separate experiment. But since this was done by opening the refrigerator, the heat from the speaker would have more easily dissipated than if it was in its original sealed setting (LaBounty et. al, p. 73-76). They concluded that both effects were negligible, which is possible, but a more likely scenario is that both projects had similar fundamental problems.

The point of this section isn't to disprove the effects observed by the previous project. If the same measurement techniques were used, Figure 34 could have been used as a proof of a working thermoacoustic refrigerator. Since using better measurement techniques with a very similar refrigerator showed no thermoacoustic effect, it is possible that the previous experiment had the same problem that went unnoticed. The larger point of this section is that table top thermoacoustic refrigerators of this nature may be in general very poor ones.

Conclusion

The goals for this project were to create a better thermoacoustic refrigerator by reconstructing the previous refrigerator and improving measurement techniques. The former was accomplished by putting in a more powerful speaker (our speaker had a power of 200 watts as compared with a speaker with 50 watts with the previous project) and by increasing the pressure of the working fluid, helium, inside the refrigerator. The increase in pressure, however, turned out to be a meaningless step because of the various helium leaks which created a mix of helium and air.

The advanced measurement techniques worked well. The thermocouples recorded the temperature of the hot exchanger, cold exchanger, and ambient accurately. The resonance was also measured satisfactorily; but, the process was more tedious than it should have been. A more advanced technique would automatically generate the resonant frequency for any given system.

There were two sets of experiments done. During the first set of experiments, the copper meshes along with the copper wool were used as heat exchangers. No thermoacoustic effect or a lot of temperature variation in general was observed. The second set of experiments was done using only the copper wool. Although a temperature change on both heat exchangers was observed, the change was not due to the thermoacoustic effect. The cold heat exchanger became colder because the room temperature went down. The hot exchanger became hotter because it was closer to the speaker which became very hot and eventually stopped working.

The thermoacoustic effect was not observed for this project. There were many reasons for this. The helium leakage caused the working fluid to be a mixture of air and helium and since the stack and other parts were designed to be in pure helium environment. The mixture also caused the resonance frequency to be different at different pressures. The noisy resonance measurements and non-ideal geometries also contributed to the problem.

Moreover, it is dubious whether the previous group saw any effect either. The experimental setup and procedure for both projects were very similar with the exception of the advanced measurement techniques used in this project. In fact, because of the superior parts used, this project should have seen a better thermoacoustic effect. From Figure 34, it is evident that a more primitive measurement technique could mistake the temperature difference for a thermoacoustic effect. This is especially true because the previous group did not measure the ambient temperature as frequently as they should have. Figure 35 shows that ambient room temperature can vary in a matter of minutes.

The previous point was not meant to doubt the integrity or the results obtained by the previous group. Instead, the point was to show that it is possible that table-top thermoacoustic refrigerators of this nature may be fundamentally ineffective. Furthermore, if the previous project was, in fact, unsuccessful, it would have directly affected the results of our work since we recycled a lot of the parts.

Future Work

Our recommendations to future investigations into thermoacoustic refrigerators revolve around avoiding the mistakes and failures discovered by this project. Without further testing, there is no way for us to detail what exactly caused the failure to achieve a thermoacoustic effect; however, we can elaborate on key potential reasons which should be avoided by subsequent attempts to construct a refrigerator.

The first and possibly most crucial problem may have been stack placement. According to the design specifications of Tijani, the resonance frequency used did not match our resonator dimensions, and so the stack heat exchangers were not on a pressure node and anti-node for either side. A future group should design a thermoacoustic refrigerator based around self-calculated optimization settings.

The reason that the resonance frequency did not match our resonator dimensions was caused by the mixture of air and helium in the system. Due to innumerable leaks occurring in the stack housing connections and around the speaker housing, the helium would leak out at a fast rate and would leave air inside. This mixture results in huge errors in resonance testing and, consequently, in our sound wave generated. In addition to this, only 2-3 atm of helium gas could be injected into the refrigerator before some component would fail, which is a fairly low pressure to be using when attempting to achieve the thermoacoustic effect. In order to both reduce leakage and have a TAR that can sustain high pressures, even stronger structural components, adhesives, and sealants are required to avoid a dearth of helium measurement accuracy.

The copper wool placed at either end of the stack may not have done their job. The wool was intended to carry heat to and from the stack to the outside copper tubes and to the thermocouples; but, we are skeptical that the wool has enough surface area to complete this task due to their small size. Either a new set of larger wools are needed or the entire heat exchanger part of the refrigerator must be redesigned.

The chemical adhesives utilized to fix the large diameter tube would creep over time by gravitational pull. When the TAR accidentally fell off the table, the spokes connecting the speaker broke off and had to be re-glued using JB weld. This displaced the speaker direction; which, combined with the creep, caused for non ideal geometries for the sound wave to pass down the resonator tube. In the future, it would be prudent to avoid using chemical adhesives and rely more on mechanical connections. Another way of avoiding non ideal geometries and having several smaller components would be to machine a majority of the apparatus from a single block of material.

Lastly, the previous group, as well as ours, suffered a broken speaker which we believe occurred because the extra power imposed by the amplifier caused the speaker to overheat. Either a new amplifier should be used or a speaker that can handle the wattage of the amplifier should be used to prevent another breakdown.

Bibliography

Garrett, Steven L., Thomas J. Hoffler, and David K. Perkins. "ThermoAcoustic Refrigeration." Alternative Fluorocarbons Environmental Acceptability Study (1993): 1-8.

Isentropics.org. 30 Apr. 2009 <http://mshades.free.fr/>.

LaBounty, Meghan, and Andrew Lingenfelter. DESIGN AND CONSTRUCTION OF A THERMOACOUSTIC REFRIGERATOR. Thesis. Worcester Polytechnic Institute, 2008. WPI.

Poignand, Gaelle, Bertrand Lihoreau, Pierrick Lotton, Etienne Gaviot, Michel Bruneau, and Vitaly Gusev. "Optimal acoustic fields in compact thermoacoustic refrigerators." Applied Acoustics 68 (2006): 642-59.

Russell, Daniel A., and Pontus Weibull. "Tabletop thermoacoustic refrigerator for demonstrations." Science and Mathematics Department, Kettering University (2001): 1231-233.

Swift, G.W. "Thermoacoustic engines." Condensed Matter and Thermal Physics Group (1988): 1145-180.

"Technical data for the element Copper in the Periodic Table." The Periodic Table of the Elements, Standard Form. 29 Apr. 2009 <http://www.periodictable.com/Elements/029/data.html>.

"Thermoacoustic Refrigeration at Penn State." Penn State - Graduate Program in Acoustics. 30 Apr. 2009 <http://www.acs.psu.edu/thermoacoustics/refrigeration/benandjerrys.htm>.

Tijani, M.E.H., J.C.H. Zeegers, and A.T.A.M. De Waele. "Construction and performance of a thermoacoustic refrigerator." Cryogenics 42 (2001): 59-66.

Tijani, M.E.H., J.C.H. Zeegers, and A.T.A.M. De Waele. "Design of thermoacoustic refrigerators." Cryogenics 42 (2001): 49-57.

Tijani, M.E.H., J.C.H. Zeegers, and A.T.A.M. De Waele. "The optimal stack spacing for thermoacoustic refrigeration." Cryogenics (2001): 128-33.

Tijani, M.E.H. Loudspeaker-driven thermo-acoustic refrigeration. Diss. Technische Universiteit Eindhoven, 2001. CIP-DATA LIBRARY TECHNISCHE UNIVERSITEIT EINDHOVEN.

Tu, Qiu, Qing Li, Fangzhong Guo, and Junxia Liu. "Temperature difference generated in thermo-driven thermoacoustic refrigerator." Cryogenics 43 (2003): 515-22.

Wheatley, John, T. Hoffler, G.W. Swift, and A. Migliori. "Understanding some simple phenomena in thermoacoustics with applications to acoustical heat engines." Condensed Matter and Thermal Physics Group (1983): 147-62.